

SYNTHESIS, SPECTRAL, REDOX AND CATALYTIC PROPERTIES OF MONONUCLEAR COPPER(II) COMPLEX

¹Velusamy Sathya, ²Mariappan Murali*

¹Research Scholar, ²Assistant Professor (*Corresponding Author)

^{1,2}Coordination and Bioinorganic Chemistry Research Laboratory

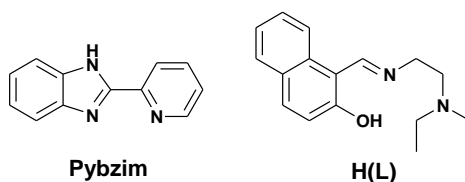
Department of Chemistry, National College (Autonomous), Tiruchirappalli 620 001
Tamil Nadu, India

Abstract : The green coloured mononuclear copper(II) complex $[Cu(L)(pybzim)](ClO_4)$ (1), where HL is tridentate Schiff base (NNO donor) ligand obtained from the condensation of 2-hydroxy-1-naphthaldehyde and N,N-diethylethylenediamine and pybzim is 2-(2-pyridyl)benzimidazole, has been synthesized and characterized. The copper(II) complex exhibits a broad band in the visible region (λ_{max} , 647 nm) and axial EPR spectra in DMF (77 K) with g_{\parallel} and A_{\parallel} values of 2.236 and $185 \times 10^{-4} \text{ cm}^{-1}$ respectively. The complex involves meridional coordination of the tridentate Schiff base ligand and possesses a CuN_4O chromophore with distorted square pyramidal geometry. It displays intermolecular noncovalent interaction as revealed by frozen solution EPR spectra in weakly coordinating solvents like MeOH and MeCN. The complex undergoes reversible $Cu(II)/Cu(I)$ redox behavior ($E_{1/2}$, +0.014 V; ΔE_p , 85 mV) in methanol solution. The electron-releasing $-NEt_2$ group as in the complex confers higher energy visible band and positive $E_{1/2}$ for the $Cu(II)/Cu(I)$ couple and enhances the stabilization of $Cu(II)$. The complex effectively catalyzes the oxidation of ascorbic acid to dehydroascorbic acid, benzylamine to benzaldehyde and 3,5-di-tert-butylcatechol to 3,5-di-tert-butyl-o-quinone, thus mimicking the function of type-2 and type-3 copper oxidases.

Keywords: Copper(II) complex, electronic spectra, EPR, redox properties, catalytic activity

I. INTRODUCTION

Copper-containing oxidases are ubiquitous in nature and have diverse and critical roles in many organisms [1-3]. It is well established that such enzymes are activated by metal ions and molecular oxygen to generate redox catalysts and involved in direct electron transfer or oxidation of various organic substrates [1,4]. Copper appears to play multiple roles in the biogenesis of these redox catalysts and in the catalytic cycles of the oxidases. Herein, we describe three exemplary copper oxidases, ascorbate oxidase (AO), amine oxidase (AmO) and catechol oxidase (CO), which utilize and activate dioxygen (O_2) during catalysis. The AO has three types of copper centers in which the type-2 site belongs to the functional trinuclear copper cluster [5]. The type-2 site has two histidines and an aqua ligand to make it three-coordinate. The key role of the type-2 copper center is electron transfer, in which ascorbate under physiological reaction conditions acts as an electron donor. The reduced $Cu(I)$ sites activate dioxygen and catalyze the four-electron reduction of dioxygen to water [6]. The AmO is a type-2 copper oxidase, exists as homodimers. The active site of each subunit consists one copper center [7] coordinated to three histidines and two water molecules in a distorted square pyramidal geometry. The role of AmO is the oxidation (two electron) of primary amines to aldehydes [8]. The CO reversibly binds to dioxygen, catalyzing the oxidation of catechols to the corresponding *o*-quinones accompanying with the four-electron reduction of O_2 to $2H_2O$ [9], is a type-3 copper protein [10] containing the dinuclear copper center, in which both copper ions are surrounded by three histidine nitrogen donor atoms [11]. The catalytic mechanism of CO reveals that both the hydroxo-bridged *met* form and the $\mu-\eta^2:\eta^2$ peroxo-bridged *oxy* forms are active in the catalytic cycle [12]. Many model complexes with dicopper center ($Cu \cdots Cu$ distance $\leq 5 \text{ \AA}$) successfully mimicking the copper oxidases [13, 14], both structurally and functionally, whereas the same for the mononuclear counterparts remain surprisingly rare. The studies disclosed that the distorted square pyramidal mononuclear copper(II) complexes acquiring labile binding sites are of great importance for modeling the active sites of copper oxidases [15, 16] and their catalytic activity has been the subject of current investigations [17]. In the present paper, we report the synthesis and properties of green coloured mononuclear copper(II) complex with NNO donor Schiff base ligand and 2-(2-pyridyl)benzimidazole (pybzim) (Scheme 1) that exhibits efficient catalytic activity towards the oxidation of ascorbic acid, benzylamine, and catechol.



Scheme 1. Structure of ligands

II. EXPERIMENTAL

2.1 Chemicals

Copper(II) acetate monohydrate, 2-(2-pyridyl)benzimidazole, 2-hydroxy-1-naphth-aldehyde, sodium perchlorate, *N,N*-diethylethylenediamine, 3,5-di-*tert*-butylcatechol, *tetra-N*-butylammonium bromide (Sigma-Aldrich), L-ascorbic acid (Fisher Scientific), benzylamine (Avra), hydrogen peroxide solution (30% w/v) (Merck) were used as received. HPLC grade methanol, *N,N*-dimethylformamide and acetonitrile and reagent grade diethyl ether were purchased from Merck.

2.2 Instruments

Microanalyses (C, H, and N) were carried out with a Vario EL elemental analyzer. The conductivity is measured using EQUIPTRONICS EQDCMP bridge with a solute concentration of 1×10^{-3} M in MeOH. Mass spectrometry was performed on a ZQ ESI-MS spectrometer. Magnetic susceptibility data at 27 °C were obtained for polycrystalline samples using George Associates Inc. FTIR spectra were recorded using a Perkin Elmer Spectrum RX1 FTIR spectrophotometer in the range 400-4000 cm^{-1} with a sample prepared as KBr disc. UV-Visible spectroscopy of reflectance spectra was recorded using Shimadzu UV-2450 UV-VIS spectrophotometer and solution spectra were recorded using Perkin Elmer Lambda-35 UV-VIS spectrophotometer using cuvettes of 1 cm path length. X-band EPR spectra of the complex in DMF at liquid nitrogen temperature (77 K) and polycrystalline at room temperature (RT) was recorded on a JEOL JES-FA200 ESR spectrometer. ^1H NMR spectra were recorded on a Bruker 300 MHz with AVANCE II NMR spectrometer in CDCl_3 . Cyclic voltammetry (CV) and differential pulse voltammetry (DPV) on glassy carbon electrode were performed in MeOH 25 ± 0.2 °C. The voltammograms were generated using CH instruments 620C electrochemical analyzer. A three electrode system has been used to study the electrochemical behaviour of complexes (0.001 M) consisting of a glassy carbon working electrode ($A = 0.0707 \text{ cm}^2$), a platinum wire auxiliary electrode and saturated calomel reference electrode and TBAP (0.1 M) is used as a supporting electrolyte. Solutions were deoxygenated by purging with nitrogen gas for 15 min prior to the measurements.

2.3 Synthesis of $[\text{Cu}(\text{L})(\text{pybzim})](\text{ClO}_4)$ (1)

To a solution of 2-(2-pyridyl)benzimidazole (pybzim; 0.19 g, 1 mmol) in MeOH (15 mL) was added $\text{Cu}(\text{O}_2\text{CMe})_2 \cdot \text{H}_2\text{O}$ (0.20 g, 1 mmol) and the blue mixture was stirred for 1 h at 25 °C at which point the yellow solution of Schiff base (HL), obtained from the condensation of 2-hydroxy-1-naphthaldehyde (0.17 g, 1 mmol) and *N,N*-diethylethylenediamine (0.12 g, 1 mmol), was added. The resultant green solution was refluxed for 3 h. The green solids obtained after the addition of a methanolic solution of NaClO_4 (0.122 g, 1 mmol) were filtered and dried *in vacuo* over P_4O_{10} . Yield: 0.46 g (73 %). Anal. Calcd. for $\text{C}_{29}\text{H}_{30}\text{N}_5\text{O}_5\text{ClCu}$: C, 55.50; H, 4.82; N, 11.16 %. Found: C, 55.46; H, 4.79; N 11.21 %. A_M (MeOH): $72 \Omega^{-1} \text{ cm}^2 \text{ mol}^{-1}$. ESI-MS (MeCN): m/z 527.11 [$\text{M}^+ - \text{ClO}_4$]. μ_{eff} (27 °C): 1.84 μB . FT-IR (KBr, cm^{-1}) selected bands: 1621 $\nu_{\text{bzim}}(\text{C}=\text{N})$; 1439 $\nu_{\text{bzim}}(-\text{C}=\text{N}-\text{C}=\text{C}-)$; 1597 $\nu_{\text{imine}}(\text{C}=\text{N})$; 1538 $\nu_{\text{py}}(\text{C}=\text{N})$; 1302 $\nu(\text{naph}-\text{O})$; 1104, 623 $\nu(\text{ClO}_4^-)$. Electronic spectrum in solid/MeOH [$\lambda_{\text{max}}/\text{nm}$ ($\epsilon_{\text{max}}/\text{dm}^3 \text{ mol}^{-1} \text{ cm}^{-1}$): 655/647 (184), 391 (6845), 308 (40971). Electronic spectrum in MeOH:H₂O (4:1 v/v) [$\lambda_{\text{max}}/\text{nm}$ ($\epsilon_{\text{max}}/\text{dm}^3 \text{ mol}^{-1} \text{ cm}^{-1}$): 651 (192), 384 (7240), 308 (43600). Polycrystalline EPR spectrum at RT: $g_{\parallel} = 2.197$, $g_{\perp} = 2.084$. EPR spectrum in DMF solution at 77 K: $g_{\parallel} = 2.236$, $g_{\perp} = 2.049$, $A_{\parallel} = 185 \times 10^{-4} \text{ cm}^{-1}$, $g_{\parallel}/A_{\parallel} = 121 \text{ cm}$, $G = 5.0$, $\alpha^2 = 0.80$, $\beta = 0.67$, $\gamma^2 = 0.55$, $K_{\parallel} = 0.73$, $K_{\perp} = 0.66$. Redox behavior in MeOH (0.1 M TBAP): CV, $E_{1/2} = 0.014 \text{ V}$, $\Delta E_p = 85 \text{ mV}$, $i_{pa}/i_{pc} = 2.0$ (decreases towards unity with increase in scan rate), $D = 6.2 \times 10^{-6} \text{ cm}^2 \text{ s}^{-1}$; DPV, $E_{1/2} = 0.025 \text{ V}$.

2.4 Ascorbic acid oxidation

The ascorbate oxidase activity of the complex is evaluated by reaction with **1** (3×10^{-3} M) and different concentration of ascorbic acid (H_2A). The experiments were run under aerobic conditions in MeOH:H₂O (4:1 v/v) medium and monitored using UV-Vis spectroscopy.

2.5 Benzylamine oxidation

The catalytic action of **1** (1×10^{-3} M) in the H_2O_2 (1 ml of 30% w/v) dependent deamination of benzylamine (100×10^{-3} M) in 10 ml MeOH:H₂O (4:1 v/v) results in the oxidation of benzylamine to benzaldehyde. The organic products were isolated from the reaction mixture by solvent extraction with diethyl ether after removal of methanol. Diethyl ether was removed by rotary evaporation and the residue was dissolved in CDCl_3 for ^1H NMR measurements.

2.6 Kinetics of 3,5-di-*tert*-butylcatechol oxidation

To determine the catecholase activity, the methanolic solution of copper(II) complex (2.9×10^{-5} M) was treated with 50 equivalents of 3,5-di-*tert*-butylcatechol (3,5-DTBC) in methanol under aerobic condition. The UV spectra of solutions were recorded directly after the addition and subsequently after regular intervals of 30 min and absorption value at 391 nm were measured as a function of time over a period of 3 h. To determine the dependence of the rates on the substrate concentration and various kinetic parameters, solution of copper(II) complex was treated with 5-45 equivalents of 3,5-DTBC.

To detect the formation of hydrogen peroxide during the catalytic reaction, reaction mixtures were prepared as in the kinetic experiments. During the course of the oxidation reaction, the solution was acidified with H_2SO_4 to pH 2 to stop further oxidation after a certain time and an equal volume of water was added. The formed quinone was extracted three times with dichloromethane. To the aqueous layer were added 1 mL of a 10% solution of KI and three drops of a 3% solution of ammonium molybdate. The formation of I_3^- could be monitored spectrophotometrically because of the development of the characteristic I_3^- band ($\lambda = 353 \text{ nm}$, $\epsilon = 26000 \text{ M}^{-1} \text{ cm}^{-1}$).

III. RESULTS AND DISCUSSION

3.1 Synthesis

Mixed-ligand copper(II) complex (**1**) of asymmetric heterocyclic NN-donor ligand 2-(2-pyridyl)benzimidazole (pybzim) and tridentate NNO-donor Schiff bases (HL is obtained by the condensation of 2-hydroxy-1-naphthaldehyde and N,N-diethylethylenediamine) has been isolated. The stoichiometry of **1** was derived from the elemental analysis. The ESI-MS data reveal that the complex retains its identity in solution and this is supported by the value of molar conductivity in methanol ($72 \Omega^{-1} \text{ cm}^2 \text{ mol}^{-1}$), which falls in the range [18] for 1:1 electrolyte. The infrared spectra of the complex exhibits most important stretching bands due to $\nu_{\text{bzim}}(\text{C}=\text{N})$ (1621 cm^{-1}) and $\nu_{\text{bzim}}(-\text{C}=\text{N}-\text{C}=\text{C}-)$ (1439 cm^{-1}), $\nu_{\text{imine}}(\text{C}=\text{N})$ (1597 cm^{-1}), $\nu_{\text{py}}(\text{C}=\text{N})$ (1538 cm^{-1}) and $\nu(\text{naph-O})$ (1302 cm^{-1}) [19, 20], ascribing the coordination of benzimidazole, imine and pyridine nitrogen and naphtholate oxygen donors to copper(II). A broad intense band (1104 cm^{-1}) and a strong sharp band (623 cm^{-1}) [21] are observed, which are typical of non-coordinated perchlorate ion. The observed value of μ_{eff} ($1.84 \mu\text{B}$) for **1** is characteristic of paramagnetic, Cu(II) mononuclear species with d^9 configuration [22].

3.2 Electronic properties

The solid-state reflectance spectrum of **1** exhibit only one broad ligand field band in the visible region (655 nm), which is characteristic of five coordinated copper(II) complex present in a distorted square pyramidal geometry [23]. On the dissolution of **1** in methanol and methanol:water (4:1 v/v) only one visible band was observed at 647 nm and 651 nm respectively with very low absorptivity (ϵ_{max} : MeOH, 184; MeOH:H₂O, $192 \text{ M}^{-1} \text{ cm}^{-1}$). There is no significant change in the low-energy ligand field band of **1** on dissolution suggesting that the distorted square pyramidal geometry is maintained in solution. The observation of the naphtholate anion to Cu(II) ligand-to-metal charge transfer (LMCT) transition as an intense band at 391 nm (ϵ_{max} , $6845 \text{ M}^{-1} \text{ cm}^{-1}$) for **1** reveals the involvement of the naphtholate oxygen in coordination in solution [24]. The intense absorption band observed in the UV region (308 nm) is attributed to the intraligand $\pi \rightarrow \pi^*$ transition located on the coordinated Schiff base and pybzim ligands. In order to probe the solution stability of **1**, we have performed electronic absorption spectral measurement for 5 mM solution of the complex at room temperature at various time intervals. The ligand field band in the visible region at 647 nm remained unaffected over a period of seven days revealing that the complex is stable at room temperature.

3.3 EPR spectral properties

The EPR spectrum of **1** exhibit one broad singlet ($g_{\text{iso}} = 2.084$) in the polycrystalline state at 298 K arising from dipolar broadening and enhanced spin lattice relaxation. In frozen solutions of **1** three of the four parallel hyperfine features were well separated while the fourth one overlapped with the perpendicular features in DMF (Fig. 1a) whereas the parallel feature was very weakly resolved and the perpendicular feature was moderately broader in MeOH (g_{iso} , 2.052; Fig. 1b) and in MeCN (g_{iso} , 2.087; Fig. 1c). These observations are consistent with the presence of dimeric intermolecular noncovalent interaction in weak coordinating solvents like MeOH and MeCN [25] while strong coordinating solvent like DMF, the interaction is disturbed due to solvolysis.

The frozen DMF solution EPR spectra of the complexes are axial with $g_{\parallel} > g_{\perp} > 2.0$ suggesting the presence of a $d_{x^2-y^2}$ ground state for copper(II) located in square-based geometry [26-28]. The bonding coefficient α^2 , is a measure of covalency of the in-plane σ -bonding evaluated using the expression $\alpha^2 = A_{\parallel} / 0.036 + (g_{\parallel} - 2.0023) + 3/7 (g_{\perp} - 2.0023) + 0.04$ [29]. The simplified expressions such as $K_{\parallel}^2 = (g_{\parallel} - 2.0023) E_{d-d} / 8\lambda_0$, $K_{\perp}^2 = (g_{\perp} - 2.0023) E_{d-d} / 2\lambda_0$, $K_{\parallel}^2 = \alpha^2 \beta^2$ and $K_{\perp}^2 = \alpha^2 \gamma^2$ (where β^2 and γ^2 are in-plane π bonds and out-of-plane π bonds respectively, K_{\parallel} and K_{\perp} are orbital reduction factors and λ_0 (-828 cm^{-1}) represents the one electron spin-orbit coupling constant) were used to calculate the bonding parameters [30]. The α^2 (0.80) and β^2 (0.67) values indicate that there is a substantial interaction in the in-plane σ -bonding whereas the in-plane π -bonding is almost covalent. The lower value of β^2 compared to α^2 indicates that the in-plane π -bonding is more covalent than the in-plane σ -bonding. The α^2 value for **1** indicates a considerable covalency in the bonding between the copper(II) ion and the ligand. For complex **1**, it is observed that $K_{\parallel} > K_{\perp}$ [31] (K_{\parallel} , 0.73; K_{\perp} , 0.66), showing the significant out-of-plane π -bonding. The g values are related by the expression, $G = (g_{\parallel} - 2) / (g_{\perp} - 2)$, if $G > 4.0$, no exchange interaction, while $G < 4.0$ reveals exchange coupling. The values of the exchange coupling parameter G (5.0), estimated from frozen solution EPR spectrum **1** was >4.0 , suggesting the absence of spin-exchange interaction between copper(II) ion in the complex in solution at 77 K. It is well known that a geometric distortion away from square planar geometry leads to an increase in g_{\parallel} and decrease in A_{\parallel} values. Also a planar CuN_4 chromophore is expected [32] to show a ligand field band at lower wavelength and g_{\parallel} and A_{\parallel} values are around 2.200 and $200 \times 10^{-4} \text{ cm}^{-1}$ respectively and the replacement of a nitrogen atom in this chromophore by an oxygen atom has been found to increase the g_{\parallel} and decrease the A_{\parallel} values [33]. The incorporation of strong axial interaction, as in the present complex, would increase the g_{\parallel} and decrease the A_{\parallel} values. Therefore, the observed g_{\parallel} (2.236) and A_{\parallel} ($185 \times 10^{-4} \text{ cm}^{-1}$) values are consistent with the presence of a strongly distorted CuN_4O chromophore in solution. The $g_{\parallel}/A_{\parallel}$ value (121 cm) falls within the range (105-135 cm) expected for complexes with square planar geometry [28] suggests that there is significant distortion from planarity.

3.4 Redox properties

The electron transfer behavior of **1** was studied by cyclic and differential pulse voltammetric technique (Fig. 2) using glassy carbon working electrode in methanol (MeOH) and 0.1 M TBAP. The complex shows a cathodic wave (E_{pc} , -0.029 V versus SCE) in MeOH corresponding to Cu(II) to Cu(I) reduction. During the reverse scan the oxidation of Cu(I) to Cu(II) occurs in the potential at $+0.056 \text{ V}$. The complex exhibits an essentially reversible cyclic voltammetric response observed at $+0.014 \text{ V}$ ($\Delta E_p = 85 \text{ mV}$ at 50 mV s^{-1} scan rate) due to the Cu(II)/Cu(I) redox behaviour as evident from the linearity of plots of i_{pc} versus $v^{1/2}$ (D ,

$6.2 \times 10^{-6} \text{ cm}^2 \text{ s}^{-1}$) and the observed values of the ratio of peak currents ($i_{pa}/i_{pc} \sim 2.0$). The positive Cu(II)/Cu(I) redox potentials indicate that the geometrical distortion induced by the sterically hindering N,N-donor pybzim chelating ligand tends to destabilize copper(II) [34]. The relatively low ΔE_p values illustrate that the structural reorganization between copper(II) and copper(I) species is minimal leading to facile electron transfer, possibly due to bulky bzim, flexible six-membered chelate ring and steric crowding by the $-\text{NEt}_2$ moiety. The Cu(II)/Cu(I) redox couple observed at +0.025 V in the differential pulse voltammetric studies.

In aqueous MeOH, the Cu(II)/Cu(I) couple is observed at -0.082 V, indicating better stability of the cupric state in the aqueous medium. The large separation of the peaks ($\Delta E_p = 123 \text{ mV}$ at 50 mV s^{-1}) and i_{pa}/i_{pc} ratio (1.4) indicate poor reversibility of the electron transfer process, which is expected for the electroprotic reaction in an aqueous medium and the site of protonation could be the naphtholato group of the Schiff base ligand. The aqueous MeOH solution is likely to favor a redox reaction in which $[\text{Cu(II)(L)(pybzim)}]^+$ could undergo conversion to a protonated species, $[\text{Cu(I)(HL)(pybzim)}]^+$, is unlikely to occur in a non-aqueous medium. The less reversibility of the Cu(II)/Cu(I) redox process is due to major structural reorganization associated with the protonation of the copper(II) species and for the possibility of having a chemical conversion of the reduced species by an ECE mechanism [35].

3.5 Oxidation of Ascorbic acid

The catalyst **1** ($3 \times 10^{-3} \text{ M}$) reacts readily with ascorbic acid (H_2A) in aqueous methanol, the initial green solution attributed to the copper(II) complex (λ_{max} , 651 nm) changed to form an unstable brown copper(I) species and new CT band (λ_{max} , 432 nm) is formed [17]. Brown color of the solution changes to the green color within a precise time period on exposure to air coincidentally with decreasing in absorption of CT band and also the reappearance of the d-d band (λ_{max} , 642 nm), which displays the gradual conversion of Cu(I) to Cu(II), using dioxygen as an oxidant (Fig. 3). The catalytic oxidation of H_2A to dehydroascorbic acid (dA) is found to be effective at $[\text{H}_2\text{A}]:[\text{complex}]$ mole ratio of 70:1. Further, the electrochemical oxidation of H_2A in the absence of **1**, an irreversible oxidation peak was observed at 0.57 V with a current of 40 μA . Upon addition of **1**, the oxidation peak changed to 0.41 V and the current enhanced to 48 μA (Fig. 4). The significant increase in the peak current and the decreasing of overpotential gave apparent proof of the catalytic effect of copper(II) complex towards H_2A [36].

3.6 Deamination reaction

Catalytic action of **1** ($1 \times 10^{-3} \text{ M}$) is found to be effective in the oxidation of benzylamine ($100 \times 10^{-3} \text{ M}$) to benzaldehyde in the presence of H_2O_2 (1 ml of 30% w/v) in 10 ml MeOH: H_2O (4:1 v/v) [37]. Reactions of the complexes with only benzylamine or reactions of benzylamine with H_2O_2 in the absence of the complex do not show any detectable formation of benzaldehyde. The organic products were separated and the residue was dissolved in CDCl_3 for ^1H NMR spectral measurements, which confirms the oxidation of benzylamine ($-\text{CH}_2-$, δ 3.872 ppm) to benzaldehyde ($-\text{CHO}$, δ 10.031 ppm) ($\text{RCH}_2\text{NH}_2 \rightarrow \text{RCHO} + \text{NH}_3$). It is also evidenced by the ESI-MS studies showing two peaks at 105.4 (m/z) and 106.2 (m/z) assignable to PhCO^+ and PhCHO respectively. Addition of benzylamine to the solution of **1** shows significant shift (λ_{max} , 651 to 722 nm) of the visible band to a lower energy (Fig. 5) revealing the formation of an octahedral copper(II) adduct. These adduct species reacts with H_2O_2 to form a brown colour solution that does not show any d-d band. It indicates the formation of copper(I) species along with the concomitant protonation of the L ligand by benzylamine adducts with copper, which undergoes oxidation to benzylimine followed by the hydrolysis of benzylimine to benzaldehyde in the presence of water.

3.7 Oxidation of catechol

The complex ($2.9 \times 10^{-5} \text{ M}$) shows significant catalytic activity towards a convenient model substrate, 3,5-di-*tert*-butylcatechol (3,5-DTBC; 50 equivalent), using aerial oxygen as an oxidant in methanol [38] due to satisfactory solubility of both the substrate (3,5-DTBC) and its product 3,5-di-*tert*-butyl-*o*-quinone (3,5-DTBQ) in the methanol solvent. The oxidation of 3,5-DTBC to the corresponding quinone 3,5-DTBQ was repetitively monitored by the growth of the strong absorption band at 391 nm recorded every 30 min time interval during the course of the reaction (Fig. 6). The experiment unequivocally proves oxidation of 3,5-DTBC to 3,5-DTBQ catalyzed by **1**. The product 3,5-DTBQ was purified by column chromatography using 10% mixture of ethyl acetate and hexane as eluent and isolated in significant yield (55.4 %). The isolated *o*-quinone was identified by comparing its melting point to that reported in the literature [39]. Also, the ^1H NMR experiments in CDCl_3 on the product confirmed the formation of 3,5-DTBQ ($-\text{CH}_3$, s, δ 1.227 ppm, 9H; $-\text{CH}_3$, s, δ 1.275 ppm, 9H; H, s, δ 6.224 ppm, 1H; H, s, δ 6.932 ppm, 1H). In order to determine the kinetic parameters for the oxidation of 3,5-DTBC (5-45 equivalents) by **1** ($2.9 \times 10^{-5} \text{ M}$), the Michaelis-Menten approach for enzyme kinetics was applied. The initial rates of the reaction were determined by monitoring the absorption at 391 nm for the first 3 h using the slope of the tangent to the absorbance versus time curve at $t = 0$. A linear relationship for the initial rates and the concentration was observed for **1** and subsequent Lineweaver-Burk plot (Fig. 7) yielding the kinetic parameters such as maximum velocity (V_{max} , $5.3 \times 10^{-4} \text{ M min}^{-1}$), Michaelis binding constant (K_M , $4.7 \times 10^{-5} \text{ M}$) and the turnover number (k_{cat} , 1100 h^{-1}). Quite interestingly, **1** shows superior activity compared to the other mono and binuclear complexes (k_{cat} , 33-925 h^{-1}) [40]. The aerial oxygen, that oxidizes 3,5-DTBC to 3,5-DTBQ in this process, is converted to H_2O_2 . H_2O_2 thus liberated was identified and characterized spectrophotometrically [41].

IV. CONCLUSION

The monomeric copper(II) complex was isolated and characterized. It possesses distorted square pyramidal geometry with CuN_4O chromophore and displays intermolecular noncovalent interaction even in solution. The complex is active in ascorbate oxidation in the presence of dioxygen. The reaction is effective to a mole ratio of ascorbic acid to the complex as 70:1. It is also effective in the deamination reaction, in which benzylamine undergoes oxidation to benzaldehyde in presence of hydrogen

peroxide. Further, it exhibits catechol oxidation as evidenced by the oxidation of 3,5-DTBC with molecular oxygen to give 3,5-DTBQ with the higher turnover number. It is proposed that ascorbic acid/benzylamine/3,5-di-*tert*-butylcatechol approaches between the pairs formed due to inter-pair interaction as well as replacing the phenolate oxygen, bind the two copper(II) centers to facilitate the electron transfer. It is clear that the catalytic activity of the complex is found to be higher like other reported mononuclear copper(II) complexes and close to that of some binuclear complexes described in the literature. Thus, these mononuclear complex models the catalytic oxidation property of the Cu(II) sites in type-2 and type-3 copper oxidases.

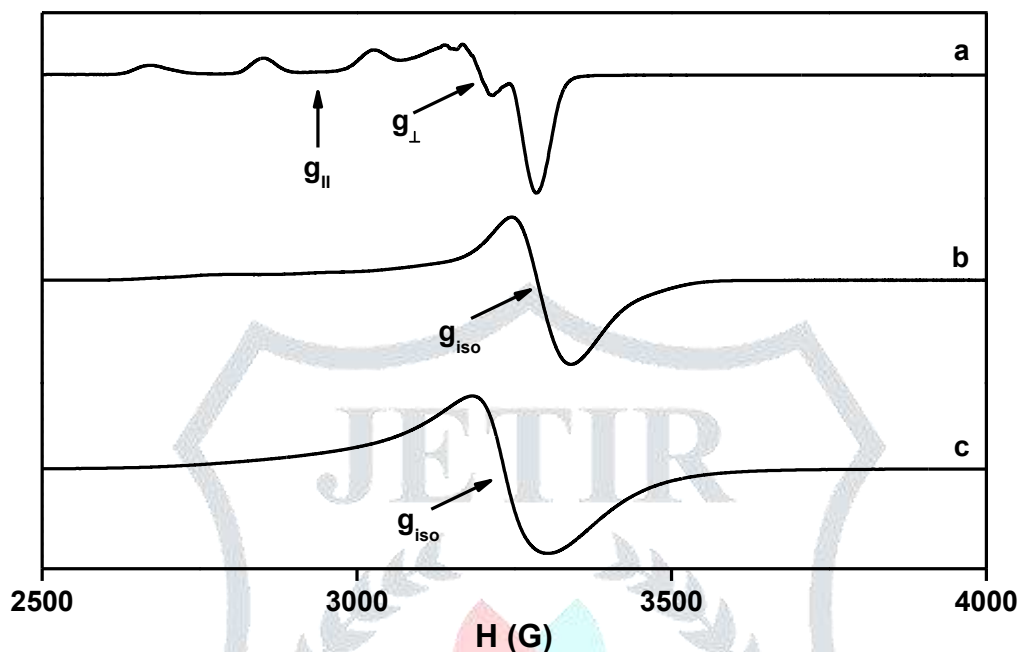


Fig. 1 EPR spectra for frozen solutions of [Cu(L)(pybzim)](ClO₄) (1) at 77K: (a) DMF, (b) MeOH and (c) MeCN.

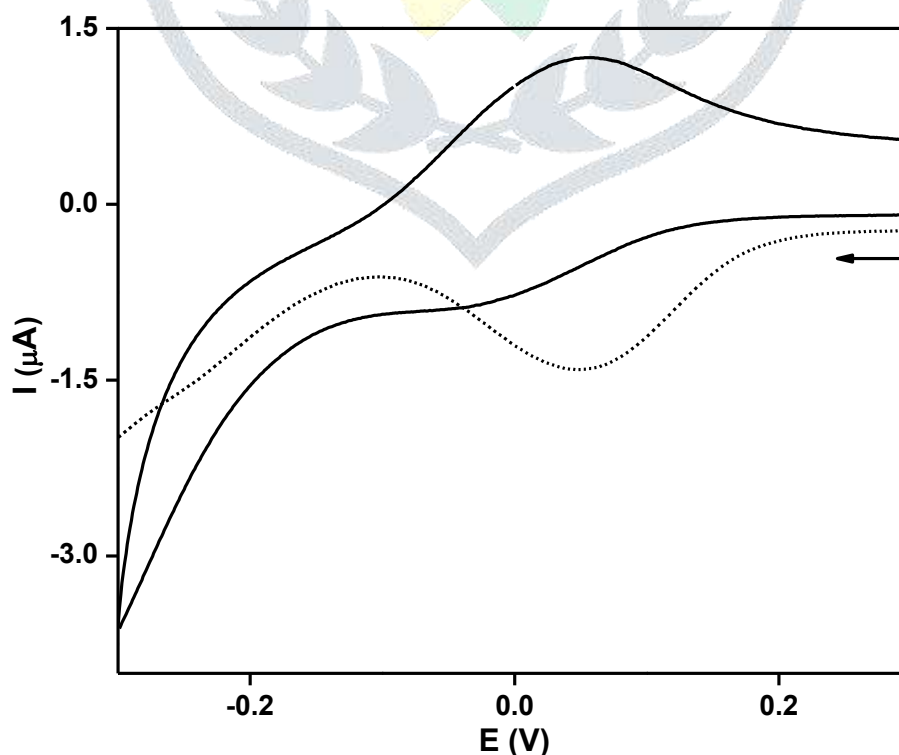


Fig. 2 Cyclic (CV) (—) and differential pulse (DPV) (-----) voltammograms of 0.001 M [Cu(L)(pybzim)](ClO₄) (1) in MeOH at 25 °C at 0.05 and 0.002 V s⁻¹ scan rates respectively.

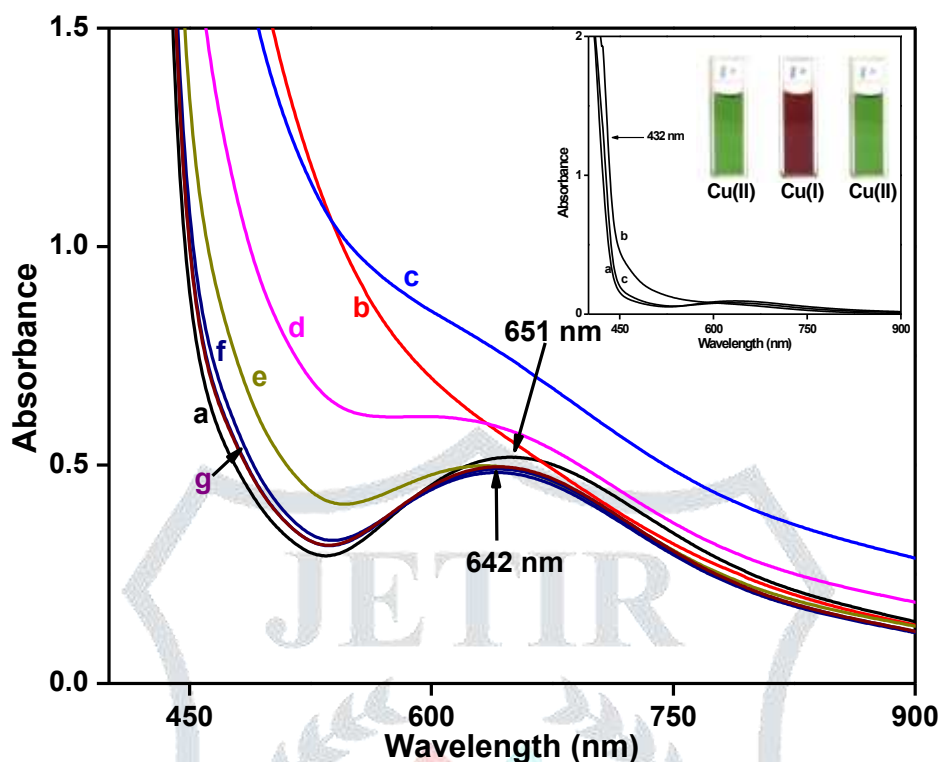


Fig. 3 Visible spectral traces showing the conversion of [Cu(L)(pybzim)](ClO₄) (1; 3 × 10⁻³ M) (a) to [Cu(HL)(pybzim)](ClO₄) (b) on reduction with ascorbic acid (3 × 10⁻³ M) in MeOH:H₂O (4:1 v/v) and the regeneration of the copper(II) species (c-g). Inset: Conversion of the copper(I) species.

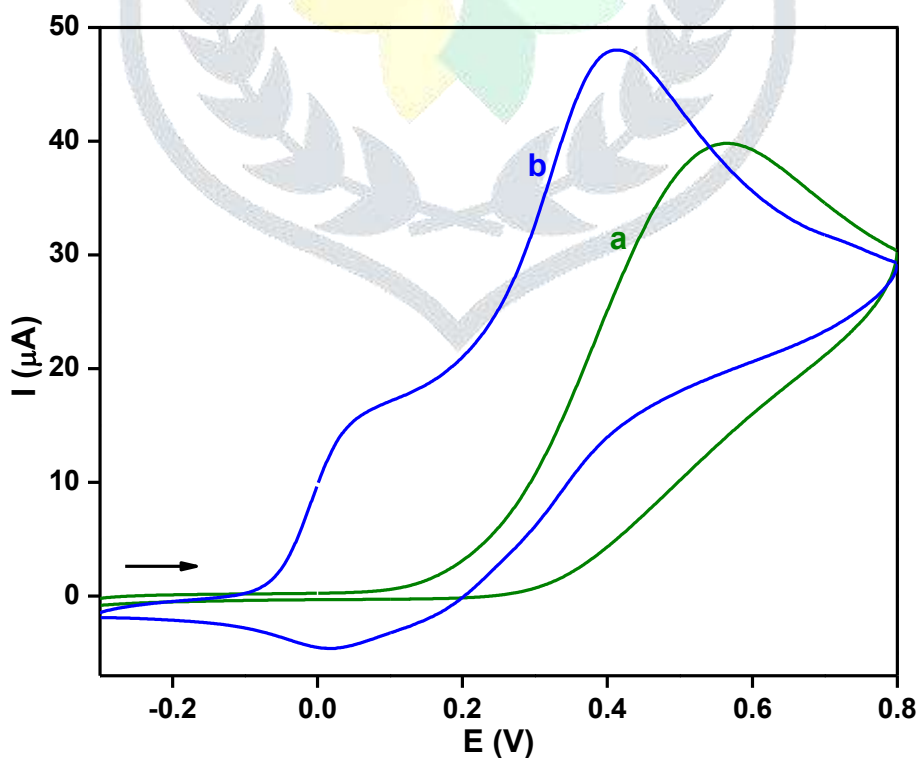


Fig. 4 Cyclic voltammograms of (a) H₂A in absence of complex and (b) H₂A in the presence of in MeOH:H₂O (4:1 v/v) (0.1 M KCl) at 0.05 V s⁻¹ scan rate.

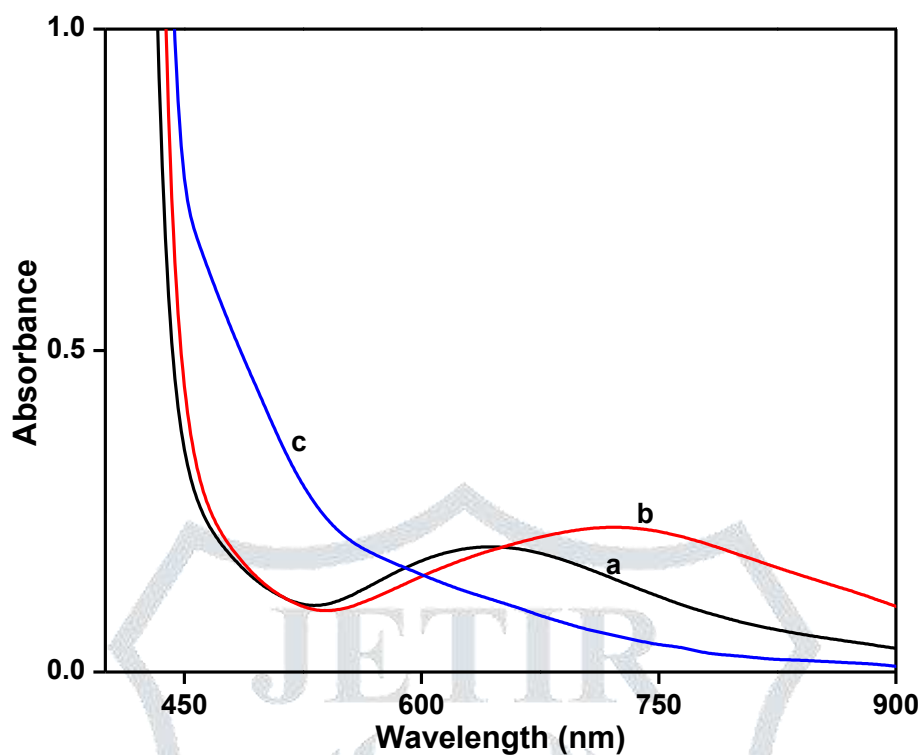


Fig. 5 Visible spectra of [Cu(L)(pybzim)](ClO₄) (**1**) in MeOH:H₂O (4:1 v/v) (a), in presence of benzylamine (b) and after treatment with benzylamine and H₂O₂ (c).

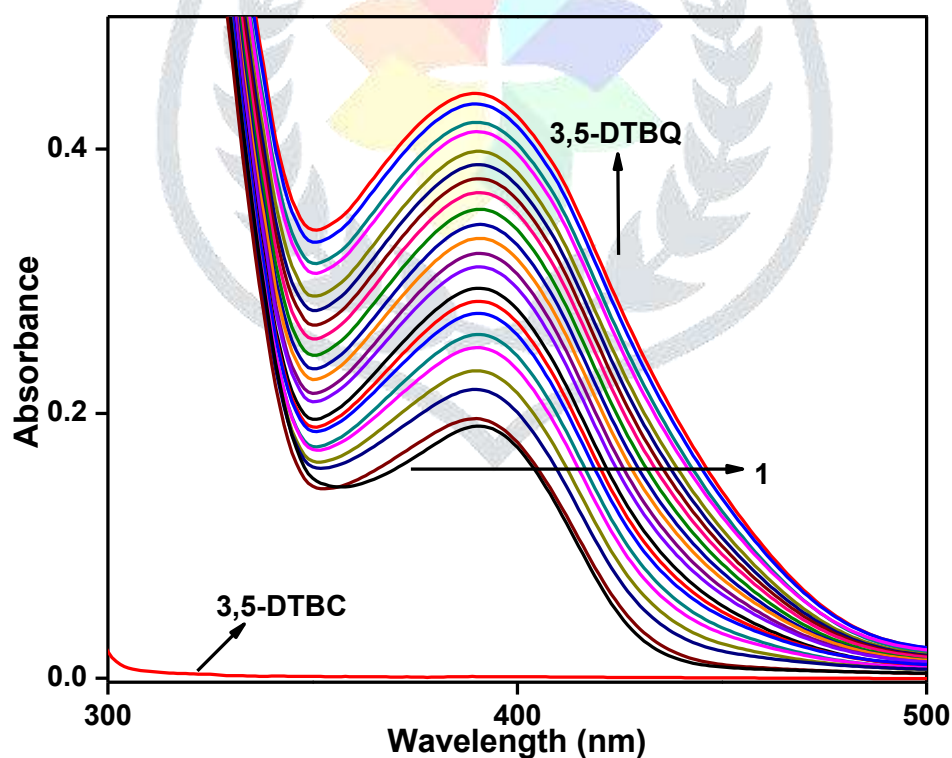


Fig. 6 Oxidation of 3,5-DTBC by [Cu(L)(pybzim)](ClO₄) (**1**) in MeOH monitored by UV-Vis spectroscopy.

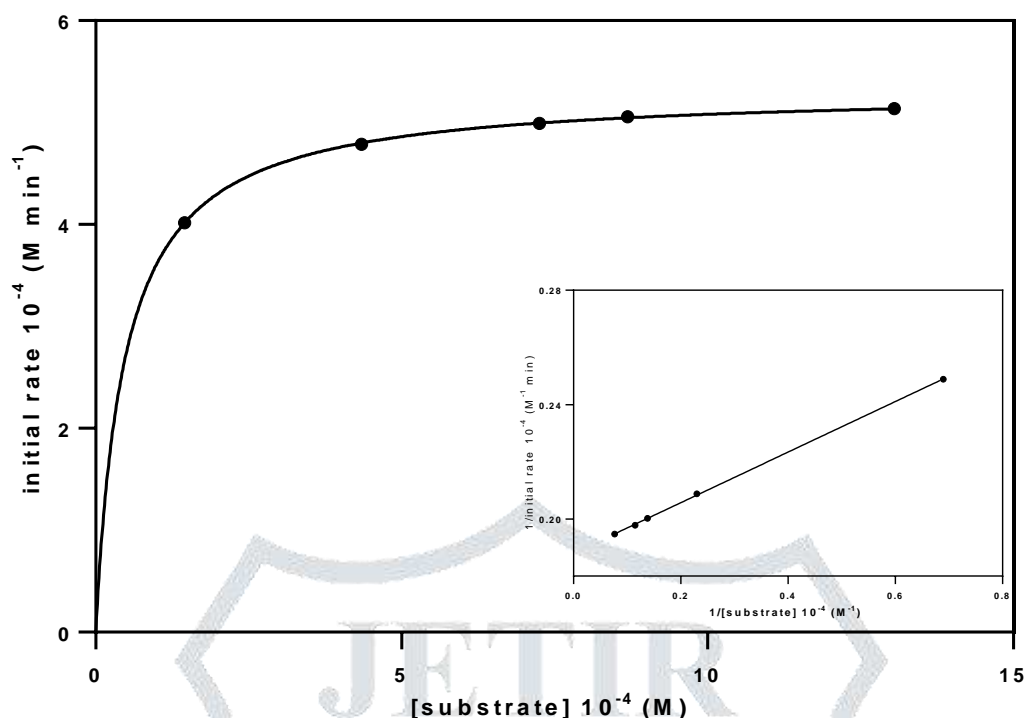


Fig. 7 Dependence of reaction rates on the 3,5-DTBC concentration for the oxidation reaction catalyzed by $[\text{Cu}(\text{L})(\text{pybzim})](\text{ClO}_4)$ (1). Inset: Lineweaver-Burk plot.

V. ACKNOWLEDGMENT

We thank the Science and Engineering Research Board, New Delhi (Grant No. EMR/2016/007756) for the financial support. We are grateful to the DST-FIST programme of the National College (Autonomous), Tiruchirappalli. We thank SAIF, Indian Institute of Technology Madras for recording EPR spectra.

REFERENCES

- [1] Halcrow, M., Knowles, P., Phillips, S., Copper Proteins in the Transport and Activation of Dioxygen, and the Reduction of Inorganic Molecules, in Handbook on Metalloproteins, I. Bertini, A. Sigel, H. Sigel, Eds., Marcel Dekker Inc., New York, 2001, pp 709-762.
- [2] Knowles, P.F., Yadav, K.D.S., Lontie, R., Ed, Copper Proteins and Copper Enzymes, 2, CRC Press, Boca Raton, FL, 1982, pp 103-129.
- [3] Knowles, P.F., Dooley, D.M., Metal Ions in Biological Systems, Singel, H., Singel, A., Eds., Marcel Dekker Inc., New York, 1994, pp 361-403.
- [4] Whittaker, J.W., Essays Biochem., 1999, 34:155-172.
- [5] Messerschmidt, A., Rossi, A., Ladenstein, R., Huber, R., Bolognesi, M., Gatti, G., Machesini, A., Petruzzelli, R., Finazzi-Agró, A., J. Mol. Biol., 1989, 206:513-529.
- [6] Messerschmidt, A., Ladenstein, R., Huber, R., J. Mol. Biol., 1993, 230:997-1014.
- [7] Chang, C.M., Klema, V.J., Johnson, B.J., Mure, M., Klinman, J.P., Wilmot, C.M., Biochemistry, 2010, 49:2540-2550.
- [8] Parsons, M.R., Convery, M.A., Wilmot, C.M., Yadav, K.D.S., Blakeley, V., Corner, A.S., Phillips, S.E.V., McPherson, M.J., Knowles, P.F., Structure, 1995, 3:1171-1184.
- [9] Koval, I.A., Gamez, P., Belle, C., Selmeczi, K., Reedijk, J., Chem. Soc. Rev., 2006, 35:814-840.
- [10] Hughes, A.L., Immunogenetics, 1999, 49:106-114.
- [11] Solomon, E.I., Augustine, A.J., Yoon, J., Dalton Trans., 2008, 3921-3932.
- [12] Gerdemann, C., Eicken, C., Krebs, B., Acc. Chem. Res., 2002, 35:183-191.
- [13] Selmeczi, K., Réglér, M., Giorgi, M., Speier, G., Coord. Chem. Rev., 2003, 245:191-201.
- [14] Holt, B.T.O., Vance, M.A., Mirica, L.M., Heppner, D.E., Stack, T.D.P., Solomon, E.I., J. Am. Chem. Soc., 2009, 131:6421-6438.
- [15] Grigoropoulou, G., Christoforidis, K.C., Louludi, M., Deligiannakis, Y., Langmuir, 2007, 23:10407-10418.
- [16] Jiang, D., Li, X., Liu, L., Yagnik, G.B., Zhou, F., J. Phys. Chem. B, 2010, 114:4896-4903.
- [17] Moradi-Shoeili, Z., Amini, Z., Boghaei, D.M., Notash, B., Polyhedron, 2013, 53:76-82.
- [18] Geary, W.J., Coord. Chem. Rev., 1971, 7:81-122.
- [19] Zhou, Q., Yang, P., Inorg. Chim. Acta, 2006, 359:1200-1206.
- [20] Temel, H., J. Coord. Chem., 2004, 57:723-729.
- [21] Ibrahim, M.M., Ramadan, A.M., Mersal, G.A.M., El-Shazly, S.A., J. Mol. Struct., 2011, 998:1-10.

- [22] Chaviara, A.T., Kioseoglou, E.E., Pantazaki, A.A., Tsipis, A.C., Karipidis, P.A., Kyriakidis, D.A., Bolos, C.A., *J. Inorg. Biochem.*, 2008, 102:1749-1764.
- [23] Dhanalakshmi, T., Suresh, E., Palaniandavar, M., *Inorg. Chim. Acta*, 2011, 365:143-151.
- [24] Camargo, T.P., Peralta, R.A., Moreira, R., Castellano, E.E., *Inorg. Chem. Commun.*, 2013, 37:34-38.
- [25] Subramanian, P.S., Suresh, E., Dastidar, P., Waghmode, S., Srinivas, D., *Inorg. Chem.*, 2001, 40:4291-4301.
- [26] Fitzgerald, W., Hathaway, B.J., *J. Chem. Soc., Dalton Trans.*, 1981, 567-574.
- [27] Hathaway, B.J., Billing, D.E., *Coord. Chem. Rev.*, 1970, 5:143-207.
- [28] Rajarajeswari, C., Loganathan, R., Palaniandavar, M., Suresh, E., Riyasdeen, A., Akbarsha, M.A., *Dalton Trans.*, 2013, 42:8347-8363.
- [29] Figgis, B.N., *Introduction to Ligand Fields*, Interscience, New York, 1996, p. 295.
- [30] Turkan, E., Sayin, U., Erbilin, N., Pehlivanoglu, S., Erdogan, G., Tasdemir, H.U., Saf, A.O., Guler, L., Akgemci, E.G., *J. Organomet. Chem.*, 2017, 831:23-25.
- [31] Hathaway, B.J., *Copper in: Comprehensive Coordination Chemistry*, vol. 5, Pergamon Press, Oxford, 1987, pp. 533-774.
- [32] Tamil Selvi, P., Murali, M., Palaniandavar, M., Kockerling, M., Henkel, G., *Inorg. Chim. Acta*, 2002, 340:139-146.
- [33] Murali, M., Palaniandavar, M., Pandiyan, T., *Inorg. Chim. Acta*, 1994, 224:19-25.
- [34] Pandiyan, T., Palaniandavar, M., Lakshminarayanan, M., Manohar, H., *J. Chem. Soc., Dalton Trans.*, 1992, 3377-3384.
- [35] Nicholson, R.S., Shain, I., *Anal. Chem.*, 1965, 37:178-190.
- [36] Zhang, Z., Li, X., Wang, C., Zhang, C., Liu, P., Fang, T., Xiong, Y., Xu, W., *Dalton Trans.*, 2012, 41:1252-1258.
- [37] Reddy, P.A.N., Nethaji, M., Chakravarty, A.R., *Inorg. Chim. Acta*, 2002, 337:450-458.
- [38] Zippel, F., Ahlers, F., Werner, R., Haase, W., Nolting, H.-F., Krebs, B., *Inorg. Chem.*, 1996, 35:3409-3419.
- [39] Tsuruya, S., Yanai, S.-I., Masai, M., *Inorg. Chem.*, 1986, 25:141-146.
- [40] Ording-Wenker, E.C.M., Siegler, M.A., Lutz, M., Bouwman, E., *Dalton Trans.*, 2015, 44:12196-12209.
- [41] Neves, A., Rossi, L.M., Bortoluzzi, A.J., Szpoganicz, B., Wiezbicki, C., Schwingel, E., *Inorg. Chem.*, 2002, 41:1788-1794.

